ACS OMEGA

Open Access

http://pubs.acs.org/journal/acsodf

Article

pH-Responsive Deacetylated Sphingan WL Gum-Based Microgels for the Oral Delivery of Ciprofloxacin Hydrochloride

Zhenyin Huang, Hanyu Dong, Yingjie Qiu, Aiping Chang,* and Hu Zhu*

Cite This: *ACS Omega* 2024, 9, 46397−46407

Read Online

ACCESS | Metrics & More | Article Recommendations | Supporting Information

ABSTRACT: Sphingan WL gum (WL) is an extracellular polysaccharide with a carboxyl group produced by *Sphingomonas* sp. WG. Recently, we have successfully obtained deacetylated WL (DWL) with good water solubility by alkaline treatment. In this study, a DWL-based microgel (named DWLM) with semi-interpenetrating network structure was constructed for the first time and used to deliver the oral drug ciprofloxacin hydrochloride (CIP). DLS results suggested that DWLM had a dual response to pH and temperature. The *in vitro* cumulative drug release curves showed that the amount of CIP released from the microgel was higher at pH 6.8 than that at pH 3.0. Biocompatibility assessments using HEK293T showed that cell viability was 75.9 ± 1.7% at the DWLM-CIP concentration of 4 mg/mL. While, the cell viability of CIP at the same concentration was only 54.9 ± 1.0%, indicating that DWLM-CIP has good biocompatibility. Antimicrobial performance tests revealed that DWLM-CIP at a concentration of 1 mg/mL could effectively inhibit the growth of *Escherichia coli* for up to 4 days. When the concentration of DWLM-CIP reached 4 mg/mL, the growth of *Staphylococcus aureus* was effectively suppressed for up to 3 days, demonstrating the long-lasting antimicrobial efficacy of DWLM-CIP. All of these results indicate that DWL-based microgels have great potential as oral drug delivery carriers.

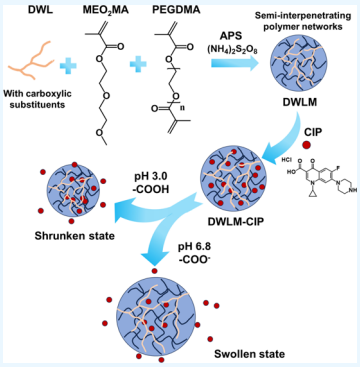

1. INTRODUCTION

Stimuli-responsive microgels have been developed as effective drug delivery systems for a variety of therapeutic, imaging, and diagnostic applications because of their tunable size, large surface area, excellent loading capacity, and high stability.[1,2] Various stimuli like pH, temperature, light, and magnetic fields have been utilized for continuous or controlled drug release through internal and external activation mechanisms.[1,2] The human gastrointestinal tract exhibits a significant pH gradient, ranging from highly acidic in the stomach (pH 1−3), through almost neutral in the small intestine, to weakly alkaline in the colon (pH 6.5−7.5).[3] These distinct pH regions in the gastrointestinal tract make pH-responsive microgels suitable candidates for oral drug delivery. In general, the volume swelling and shrinkage of pH-responsive microgels are due to deprotonation (COO^-, pH > pK_a) and protonation (COOH, pH < pK_a) of carboxyl groups in the polymer network.[4] For example, Bai et al.[5] synthesized microgels containing poly(acrylic acid) (PAA) components that collapsed in a pH 1.2 simulated gastric environment to reduce insulin release and swelled in a pH 6.8 simulated intestinal environment to facilitate its release. Rashid et al.[6] produced microgels containing itaconic acid that reduced esomeprazole release at pH 1.2, simulating the stomach, and swelled at intestinal pH levels (6.5 and 7.4) to enhance release. It is fair to say that as potential excipients, pH-responsive microgels containing carboxylic acid groups have demonstrated advantages for oral drug delivery.

Sphingan WL gum (WL), a natural microbial exopolysaccharide, is produced by *Sphingomonas* sp. WG (CCTCC No: M2013161), which was discovered by our group in the sea mud samples collected at Jiaozhou Bay.[7,8] As we reported, WL consists mainly of D-mannose, D-glucose, L-rhamnose, glucuronic acid, and O-acetyl groups, aligning closely with welan gum.[9] And the proposed structure is α-L-Rha-(1 → 4)-β-L-Rha-(1 → 4)-β-D-Glc-(1 → 3)-α-D-Glc with β-D-Man substituent on the third glucose residue and carboxyl and O-acyl groups. Since the discovery of WL, we and our collaborators have conducted extensive and in-depth research on its structure, properties, and applications.[10−16] In 2022, citric acid-cross-linked WL hydrogel wound dressing was successfully prepared, which is our first attempt to use WL in biomedicine.[10] It is worth noting that this hydrogel exhibited pH-responsive drug release properties and superior biocompatibility. Then we improved the water solubility of WL by alkali treatment and obtained deacetylated WL (DWL).[11] Compared with WL, DWL has better water solubility, which makes it have a wider application prospect.

Received: August 16, 2024
Revised: October 24, 2024
Accepted: October 28, 2024
Published: November 6, 2024

Natural polysaccharides have been widely used in the design and synthesis of stimulus-responsive microgels due to their good biocompatibility, low toxicity, and high content of active functional groups.[17−19] Therefore, in this paper, DWL with a carboxyl group was chosen for the preparation of pH-responsive microgel carrier. The good water solubility of DWL will prevent the formation of large aggregates during synthesis.[20] In addition, poly[oligo(ethylene glycol)-methacrylate] (PEGMA) components are often used as the basic building blocks of functional microgels because of their excellent biocompatibility and thermo-sensitivity.[21] Herein, DWL polymer chains were immobilized into PEGMA covalently cross-linked networks to synthesize DWL-based microgels with semi-interpenetrating networks (semi-IPN) structure. This microgel showed pH and temperature dual responsiveness. On the other hand, as a third-generation fluoroquinolone, ciprofloxacin hydrochloride (CIP) is effective in treating bacterial infections caused by Gram-positive and Gram-negative pathogens. In clinical use, CIP has shown efficacy in urinary tract infections, ulcerative colitis, and peritonitis.[22,23] However, CIP has been associated with gastric and intestinal disorders in humans.[24] It can be said that in order to reduce the frequency and side effects of oral administration, the design and development of an oral controlled/sustained-release drug delivery system is very necessary for CIP. Therefore, CIP was selected as an oral drug model for the loading and release experiments.

In this work, DWL-based microgels (named DWLM) with semi-IPN structure were prepared by the direct polymerization of monomer 2-(2-methoxyethoxy)ethyl methacrylate (MEO_2MA) and the cross-linker poly(ethylene glycol)-dimethacrylate (PEGDMA) initiated by ammonium persulfate (APS) in the DWL aqueous solution (Scheme 1). Then the model drug CIP was loaded into the microgel by physical adsorption, and the resulting microgel was named DWLM-CIP. Subsequently, the structures of DWLM and DWLM-CIP were analyzed using FTIR, UV−vis, DLS, ζ-potential, and TEM. The pH/temperature dual-stimuli-responsiveness of DWLM was investigated using DLS. Next, drug release studies of DWLM-CIP were performed in simulated gastrointestinal environments (pH 3.0 and 6.8) at 37 and 20 °C. Finally, the biocompatibility and antimicrobial activity of DWLM and DWLM-CIP were evaluated carefully. All results indicate that DWL-based microgels have a good potential as oral drug delivery carriers. This work is intended to broaden the application scope of the natural anionic polysaccharide DWL.

Scheme 1. Schematic Illustration of the Synthesis and pH-Responsive Drug Release of Deacetylated Sphingan WL Gum-Based Microgels

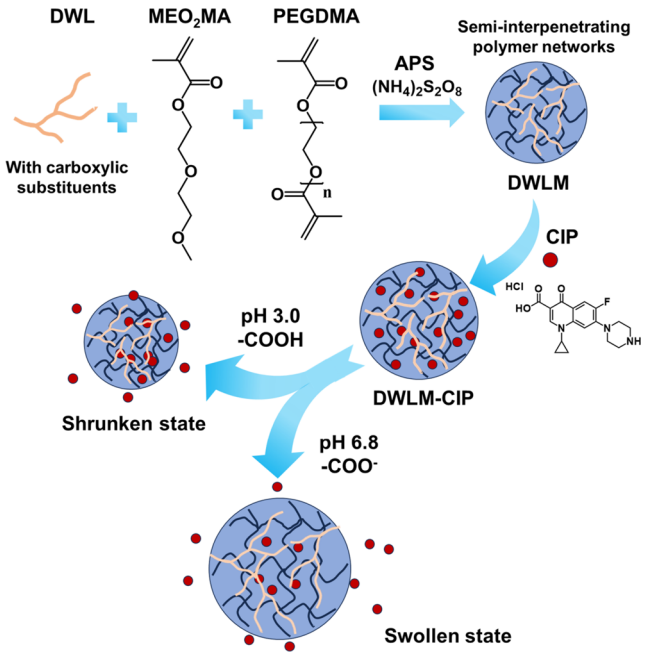

2. MATERIALS AND METHODS

2.1. Materials. Deacetylated WL (DWL) with a molecular weight of M_w = 2.70 × 10^7 Da was obtained by treating Sphingan WL gum (WL) with sodium hydroxide, as described in the published literature.[11] 2-(2-methoxyethoxy)ethyl methacrylate (MEO_2MA, 95%) and poly(ethylene glycol)-dimethacrylate (PEGDMA, M_n = 550) were offered by Sigma and further purified on neutral alumina column. Methyl thiazolyl tetrazolium (MTT, 98%) was obtained from Aladdin Biochemical. Ciprofloxacin hydrochloride (CIP, 98%) and sodium dodecyl sulfate (SDS, 95%) were supplied by Macklin Biochemical. Penicillin-streptomycin (PS), fetal bovine serum (FBS), and Dulbecco's modified Eagle's medium (DMEM) were provided by Adama's life.

2.2. Preparation of DWLM. The following microgels were synthesized by free radical precipitation polymerization. DWL (50 mg) was added to a 250 mL three-necked flask containing 100 mL of ultrapure water and dissolved overnight with thorough stirring. SDS (5 mg, 0.017 mmol), MEO_2MA (420 μL, 2.277 mmol), and PEGDMA (40 μL, 0.080 mmol) were added with stirring. Ar was passed and the temperature was raised to 70 °C for 1 h. The ammonium persulfate (APS) solution (1 mL, 0.22 mol/L) was added to initiate the polymerization, and the reaction was allowed to proceed for 5 h. The obtained microgels were purified through repetitive centrifugation (14,000 rpm, 40 °C, 30 min), decantation, and redispersion in water. Then, the microgel dispersion was dialyzed (cutoff 8000−14,000 Da) for 3 days. The final purified microgels were obtained and named DWLM. When DWL was absent in the polymerization reaction system, pure PEGMA-based microgels (named EM) were obtained. EM was synthesized as a control.

2.3. Microgel Characterization. DLS and ζ-potentials were measured using a nanoparticle size and ζ-potential analyzer (Zetasizer Nano ZSE, Malvern). The very dilute microgel dispersions were used, and each dispersion was allowed to equilibrate for at least 10 min at the measurement temperature. For the pH-sensitive assays, the pH of the microgel dispersion was adjusted to between 3 and 10 by using 0.1 M NaOH solution or 0.1 M HCl solution. ζ-potential was measured at 25 °C. Each sample was measured three times. FTIR spectral data were measured using a Thermo Scientific Nicolet IS50 spectrometer by the KBr tablet method (4000−400 cm^{-1}, 32 scans). UV−vis spectra were recorded on a TU-1810 PC spectrophotometer (Persee) (200−400 nm). TEM was performed by using a JEOL JEM-F200 electron microscope. The samples were dripped onto a copper mesh and dried at room temperature for at least 3 days.

2.4. Preparation of DWLM-CIP. A low-temperature (constant-temperature) stirring reaction bath was used for this experiment. 4 mL of DWLM aqueous dispersion (19 mg/

https://doi.org/10.1021/acsomega.4c07589
ACS Omega 2024, 9, 46397−46407

mL) was first stirred with a magneton at 4 °C for 1 h to ensure adequate swelling. Then, 1 mL of a CIP aqueous solution (7 mg/mL) was carefully introduced. The mixture was stirred for another 24 h. Then, the free drugs were removed by dialysis (cutoff 8000−14,000 Da) in water at room temperature.[25,26] The microgel loaded with CIP was obtained and named the DWLM-CIP.

The encapsulation efficiency (EE) and drug loading capacity (DLC) were measured by analyzing the values of the solution outside the dialysis tubing at 276 nm in the UV−vis spectrum. The mass of the unloaded drug was calculated from a standard curve (Figure S1) calibrated against a CIP sample of known concentration. Values are presented as the mean ± SD; $n = 3$. The EE and DLC are then given as.

$$\text{EE (wt\%)} = \frac{\text{mass of CIP loaded in microgels}}{\text{the initial mass of the CIP}} \times 100\% \quad (1)$$

$$\text{DLC (wt\%)} = \frac{\text{mass of CIP loaded in microgels}}{\text{mass of CIP loaded microgels}} \times 100\% \quad (2)$$

2.5. *In Vitro* Drug Release Test and Kinetic Studies. The release of CIP from DWLM-CIP was assessed under conditions that simulate the gastric and intestinal environments. pH 3.0 buffer was used as simulated gastric fluid by preparing acetate buffer (a mixture of acetic acid and sodium acetate) and pH 6.8 buffer was used as simulated intestinal fluid by preparing phosphate buffered saline (PBS).[27] The DWLM-CIP suspension (0.5 mL, 12.5 mg/mL) was placed in a dialysis bag (cutoff 3500 Da), which was then transferred to sample vials containing 10 mL of pH 3.0 or pH 6.8 buffer, respectively. Dialysis was performed in a thermostatically controlled shaker at 37 °C/20 °C, and shaken at 100 rpm to ensure the efficient release and diffusion of CIP. At predetermined time intervals, 1 mL of external buffer was removed from each drug release system and promptly substituted with the same amount of fresh buffer to ensure a uniform environment for the release kinetics. Based on the standard curve shown in Figure S1, the samples were gathered for analysis in order to quantify the release of CIP. The total amount of CIP released from DWLM-CIP was determined by utilizing the equation.[10]

$$\text{cumulative release (\%)} = \frac{C_t V_0 + \sum_1^{t-1} V_s C_t}{m} \times 100\% \quad (3)$$

where, C_t is the measured CIP concentration at time t, V_0 is the volume of release medium (10 mL), V_s is the sample volume (1 mL), and m is the total mass of CIP contained in the initial unreleased DWLM-CIP. Values are expressed as mean ± SD; $n = 3$.

The release kinetics of DWLM-CIP were examined *in vitro* by applying four widely utilized mathematical models to the drug release data.[28]

$$\text{zero-order model:} \quad M_t/M_\infty = k_0 t \quad (4)$$

$$\text{first-order model:} \quad \ln(1 - M_t/M_\infty) = -k_1 t \quad (5)$$

$$\text{Higuchi model:} \quad M_t/M_\infty = k_{sp} t^{0.5} \quad (6)$$

$$\text{Korsmeyer-Peppas model:} \quad M_t/M_\infty = k_{sp} t^n \quad (7)$$

k represents the release kinetic constant, while M_t/M_∞ indicates the fractional release of the drug at a given time t.

2.6. *In Vitro* Cytocompatibility Evaluation. MTT[10] assays were performed using human embryonic kidney 293T cells (HEK293T) to evaluate the *in vitro* cytotoxicity of DWLM, DWLM-CIP, and CIP. HEK293T was seeded in 96-well plates (2500 cells/well) containing 10% FBS and 1% PS in DMEM with the condition of 5% CO_2 at 37 °C. After 1 day of incubation, the supernatant of the medium was removed, and then 100 μL of different concentrations of DWLM, DWLM-CIP, and CIP were transferred to the corresponding wells. The concentrations of DWLM and DWLM-CIP were 0, 0.10, 0.25, 0.50, 1.00, 2.00, and 4.00 mg/mL, and the concentration of CIP at the same level was 0, 2.96, 7.39, 14.79, 29.58, 59.15, and 118.30 μg/mL. After the cultivation for a further 24 h, the HEK293T was washed with PBS. A new medium (100 μL) and 10 μL of MTT (5 mg/mL) were added to every well, and the cells were incubated for 4 h. The MTT solution was aspirated gradually, and then, 100 μL of DMSO was added to each well to dissolve the formazan crystals. The cell viability of the samples was assessed by measuring the absorbance at 570 nm with a microplate reader (Synergy-Lx, BioTek). The absorbance value of the control was set to 100% cell viability. Values are expressed as mean ± SD; $n = 3$.

2.7. *In Vitro* Antibacterial Activity. The antibacterial activity of DWLM, DWLM-CIP, and CIP was evaluated against Gram-negative *Escherichia coli* (*E. coli*, DH5α) and Gram-positive *Staphylococcus aureus* (*S. aureus*, CICC 10384) using the agar disc diffusion method and colony counting method. The PBS used below consisted of a pH 6.8 buffer solution. The specific operation steps were described as follows.

The strains were incubated on a shaker (37 °C, 165 rpm) for 12 h. The bacterial solution obtained was diluted to 1.0×10^8 CFU/mL. This bacterial solution was then further diluted and uniformly spread evenly on Luria−Bertani (LB) agar plates. After 15 min, four 7 mm diameter holes were made in the LB agar plates by using a sterile punch. Subsequently, DWLM (20 μL, 3.34 mg/mL), DWLM-CIP (20 μL, 3.34 mg/mL, with a CIP concentration of 100 μg/mL), CIP (20 μL, 100 μg/mL), and PBS (20 μL, control) were added to the wells and incubated for 24 h at 37 °C.

The concentration of bacteria was reduced to 1.0×10^8 CFU/mL before combining it with the measured samples. After incubating the combination of bacteria and drugs for 8 h at 37 °C, then the mixture was diluted and 100 μL was evenly distributed on LB agar plates and incubated for 24 h. The number of bacterial colonies on the agar plates was recorded. In the antimicrobial experiments against *E. coli*, the final concentrations of DWLM and DWLM-CIP were 0, 1.88, 3.75, and 7.50 μg/mL and CIP was 0, 0.06, 0.11, and 0.23 μg/mL, respectively. In addition, they were against *S. aureus*, the final concentrations of DWLM and DWLM-CIP were 0, 3.75, 7.50, and 15.00 μg/mL and CIP was 0, 0.11, 0.23, and 0.45 μg/mL, respectively.

The long-lasting antibacterial activity of the microgel was further tested. The bacterial solution was diluted to 1.0×10^5 CFU/mL. For the long-lasting antimicrobial assay of microgels against *E. coli*, 1 mL of 1 mg/mL DWLM, DWLM-CIP, and 1 mL of PBS (control) were loaded into a dialysis bag (cutoff 8000−14,000 Da) and placed in a sample vial containing 2 mL of the bacterial solution. Similarly, DWLM (1 mL, 4 mg/mL), DWLM-CIP, and 1 mL of PBS (control) were loaded into a

https://doi.org/10.1021/acsomega.4c07589
ACS Omega 2024, 9, 46397−46407

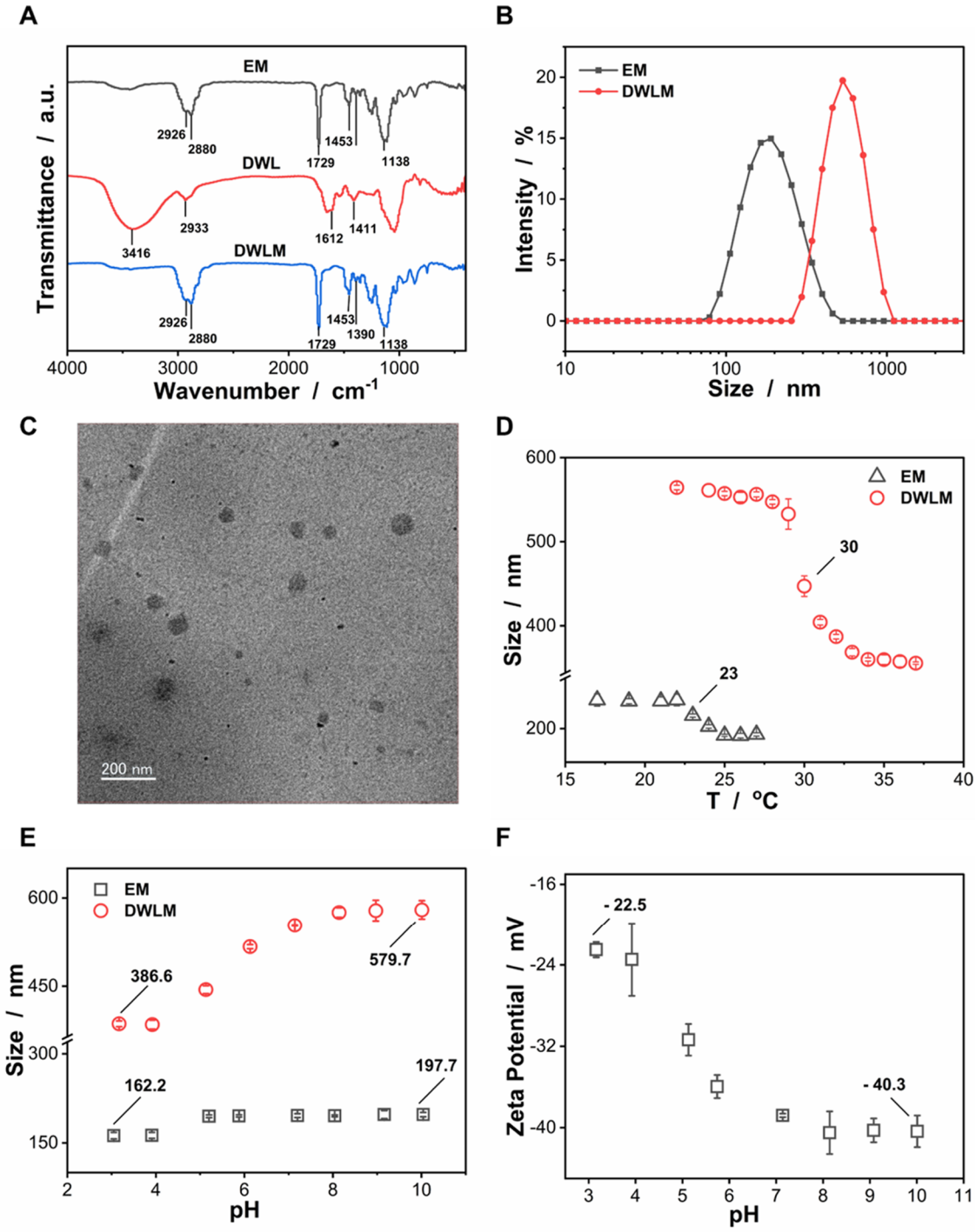

Figure 1. (A) FTIR spectra of EM, DWL, and DWLM. (B) DLS size distributions of the EM and DWLM at 25 °C. (C) TEM image of DWLM at 200 nm. (D) Temperature-dependent size values of EM and DWLM. (E) pH-Dependent size values of EM and DWLM at 25 °C. (F) ζ-Potentials of DWLM in different pH media at 25 °C. Values are expressed as the mean ± SD; n = 3.

dialysis bag and placed in a sample vial containing 2 mL of *S. aureus* solution. Following 24 h of incubation at 37 °C, 100 μL of the culture solution was spread on an LB agar plate and incubated at the same temperature for another 24 h. The medium was replaced with newly prepared bacterial suspensions every day to assess the long-lasting antibacterial effectiveness of the microgels. Colony forming units were determined by using ImageJ software. The number of colonies in the control group was defined as 100% bacterial survival. Values are expressed as mean ± SD; n = 3.

2.8. Statistical Analysis. The difference between different groups was determined by using a one-way ANOVA test. The significance levels were considered as $^{*}P < 0.05$, $^{**}P < 0.005$, and $^{***}P < 0.0005$ (vs control).

3. RESULTS AND DISCUSSION

3.1. Preparation and pH/Temperature Response of DWLM. In this study, deacetylated WL (DWL) with a good water solubility was obtained by alkaline treatment of sphingan WL gum. The absence of the acetyl C═O stretching vibration

https://doi.org/10.1021/acsomega.4c07589
ACS Omega 2024, 9, 46397−46407

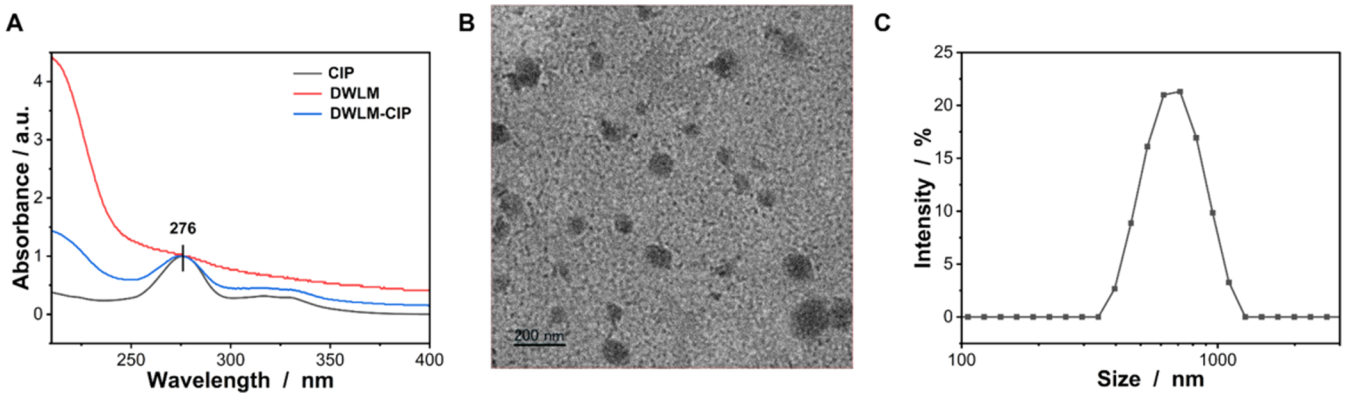

Figure 2. (A) UV−vis spectra of CIP, DWLM, and DWLM-CIP. (B) TEM image of DWLM-CIP at 200 nm. (C) DLS size distribution of DWLM-CIP at 25 °C.

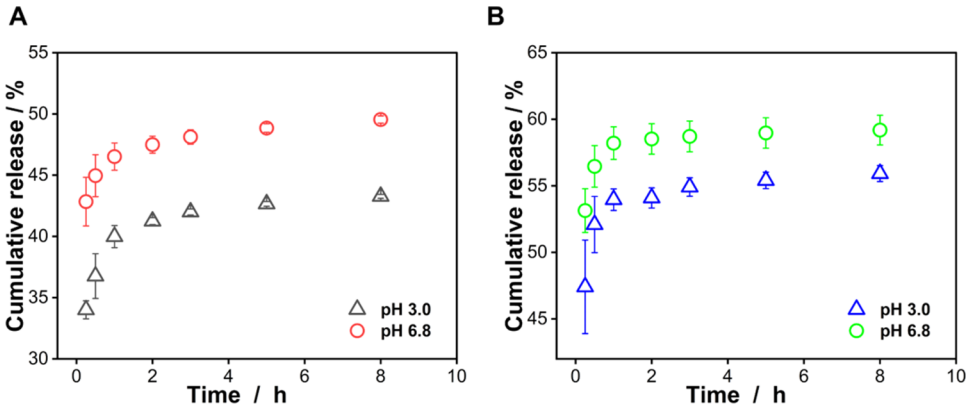

Figure 3. *In vitro* cumulative release of CIP from DWLM-CIP at different pH values over 8 h: (A) at 37 °C (B) at 20 °C. Values are presented as the mean ± SD; n = 3.

Table 1. *In Vitro* Release Kinetic Data of CIP from DWLM-CIP

	zero-order	first-order	Higuchi	Korsmeyer−Peppas	
release medium	R^2	R^2	R^2	R^2	n
pH 3.0, 37 °C	0.542	0.579	0.753	0.943	0.053
pH 6.8, 37 °C	0.579	0.459	0.796	0.975	0.034
pH 3.0, 20 °C	0.404	0.719	0.610	0.845	0.030
pH 6.8, 20 °C	0.642	0.534	0.778	0.882	0.025

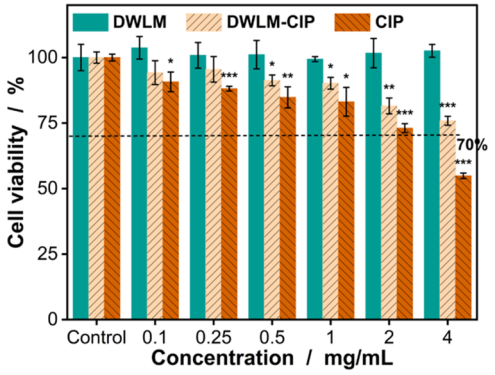

Figure 4. Cell viability of HEK293T cells in the presence of DWLM, DWLM-CIP, and CIP at different concentrations. Values are expressed as the mean ± SD; n = 3.

at 1725 cm^{-1} in the FTIR spectrum of DWL indicates the successful alkali-induced hydrolysis of the acetyl group,[11] as shown in Figure S2A. Subsequently, DWL-based microgels (named DWLM) with semi-IPN structures were prepared for the first time by radical precipitation polymerization using DWL as the raw material, MEO_2MA as the reactive monomer, and PEGDMA as the cross-linking agent. Pure PEGMA-based microgels (named EM) without DWL were synthesized as a control. The chemical composition of the microgel was examined by using FTIR spectroscopy (Figure 1A). First, for DWL obtained by alkali treatment, O−H stretching vibration was recorded at 3416 cm^{-1}, C−H stretching vibration was recorded at 2933 cm^{-1}, and COO^- stretching vibration was recorded at 1612 and 1411 cm^{-1}, showing two broad bands, indicating that alkali treatment resulted in increased deprotonation of carboxyl groups.[11] In addition, DWLM had FTIR characteristic absorption peaks that were similar to those of EM. For example, specific frequencies such as 2926, 2880 cm^{-1} (representing stretching vibrations of $-CH_2-$ and $-CH_3$), 1729 cm^{-1} (showing stretching vibrations of the ester group −OOC−), 1453, 1390 cm^{-1} (indicating bending vibrations of $-CH_2-$ and $-CH_3$), and 1138 cm^{-1} (demonstrating stretching vibrations of C−O−C) have been identified.[29] No new characteristic FTIR absorption peaks appeared after the addition of DWL. The reason could be that DWL and EM have similar FTIR absorption peaks, causing an overlap in the FTIR signal of DWL. As shown in Figure 1B, the size distributions of EM and DWLM were compared by DLS. Every microgel exhibited a tight range of particle sizes. DWLM

https://doi.org/10.1021/acsomega.4c07589
ACS Omega 2024, 9, 46397−46407

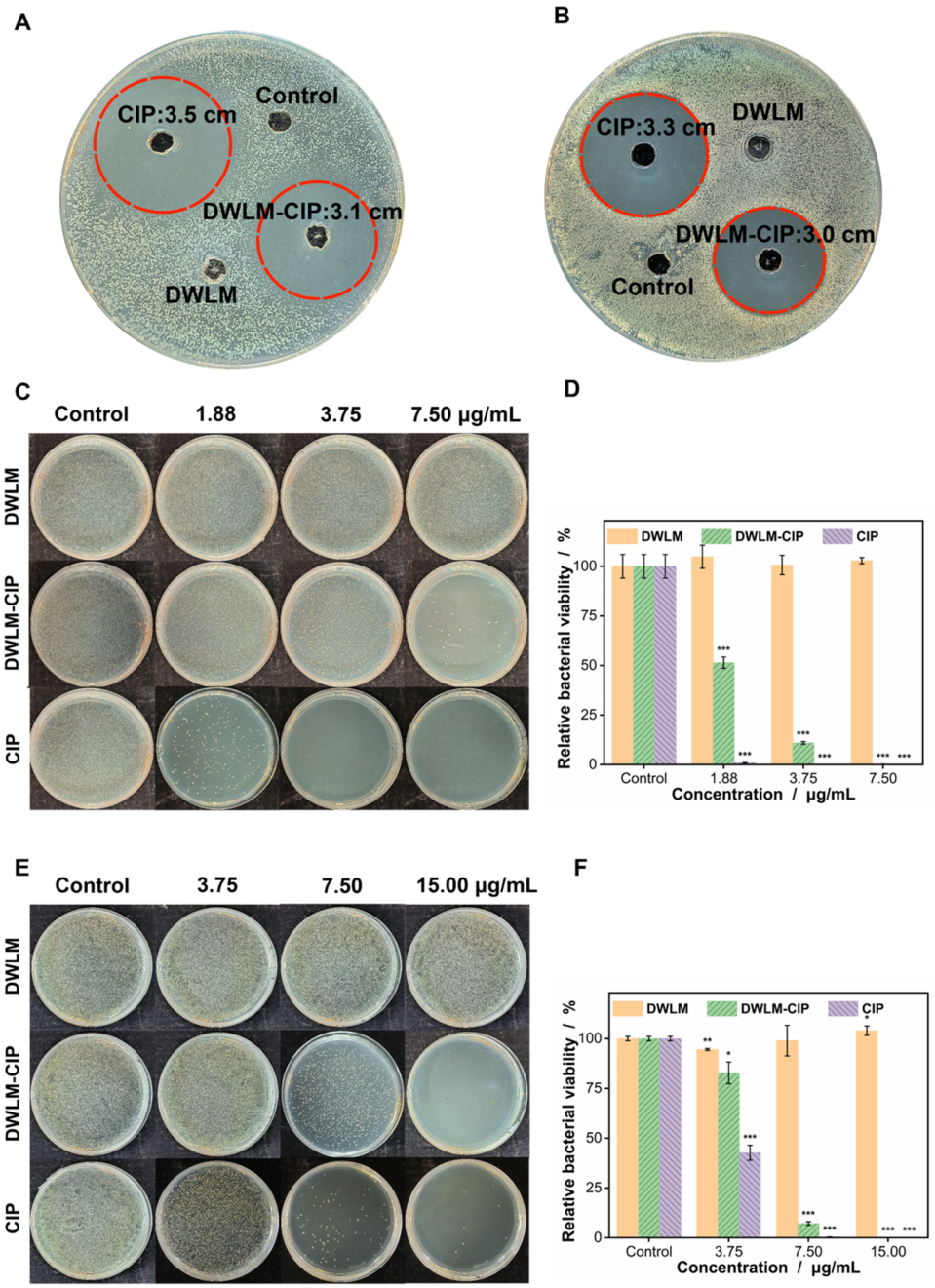

Figure 5. *In vitro* antibacterial activities of DWLM, DWLM-CIP, and CIP. Photos of inhibition zones against (A) *E. coli* and (B) *S. aureus* after 24-h incubation. Photos of bacterial colonies and corresponding bacterial viabilities formed by (C, D) *E. coli* and (E, F) *S. aureus* treated with different concentrations of DWLM, DWLM-CIP, and CIP. Values are expressed as the mean ± SD; $n = 3$.

had a larger size (557.3 ± 2.6 nm, PDI = 0.369 ± 0.018) than EM (191.9 ± 1.3 nm, PDI = 0.161 ± 0.004) at 25 °C. The increase in dimensions was credited to the effective integration of DWL into the 3D framework of the microgels. Furthermore, the spherical structure with excellent dispersion of DWLM was revealed by the TEM image (Figure 1C). The size of DWLM in the TEM image (66.8 ± 14.9 nm, Table S1) was smaller than that observed in DLS (557.3 ± 2.6 nm in Figure 1B), which can be attributed to the natural drying and dehydration of TEM samples prior to imaging. The above results indicate the successful preparation of the DWLM.

The addition of the temperature-sensitive monomer MEO_2MA rendered the synthesized microgels temperature sensitive.[21] As shown in Figure 1D, the temperature responses of EM and DWLM were evaluated by the DLS assay. The size of all microgels decreased with increasing temperature. The deswelling ratios which were the comparison of particle size ratios of EM at 27 to 17 °C and DWLM at 37 to 22 °C were 0.83 (193.0 ± 2.0 nm/233.9 ± 7.2 nm) and 0.63 (355.5 ± 1.4 nm/564.4 ± 2.7 nm), respectively. EM undergoes a volume phase transition temperature (VPTT) of approximately 23 °C, whereas DWLM experiences an elevated VPTT of 30 °C. This is because the incorporation of DWL increases the hydrophilicity of the microgels, tipping the balance toward hydrophilicity and causing the VPTT of DWLM to rise.[30]

https://doi.org/10.1021/acsomega.4c07589
ACS Omega 2024, 9, 46397−46407

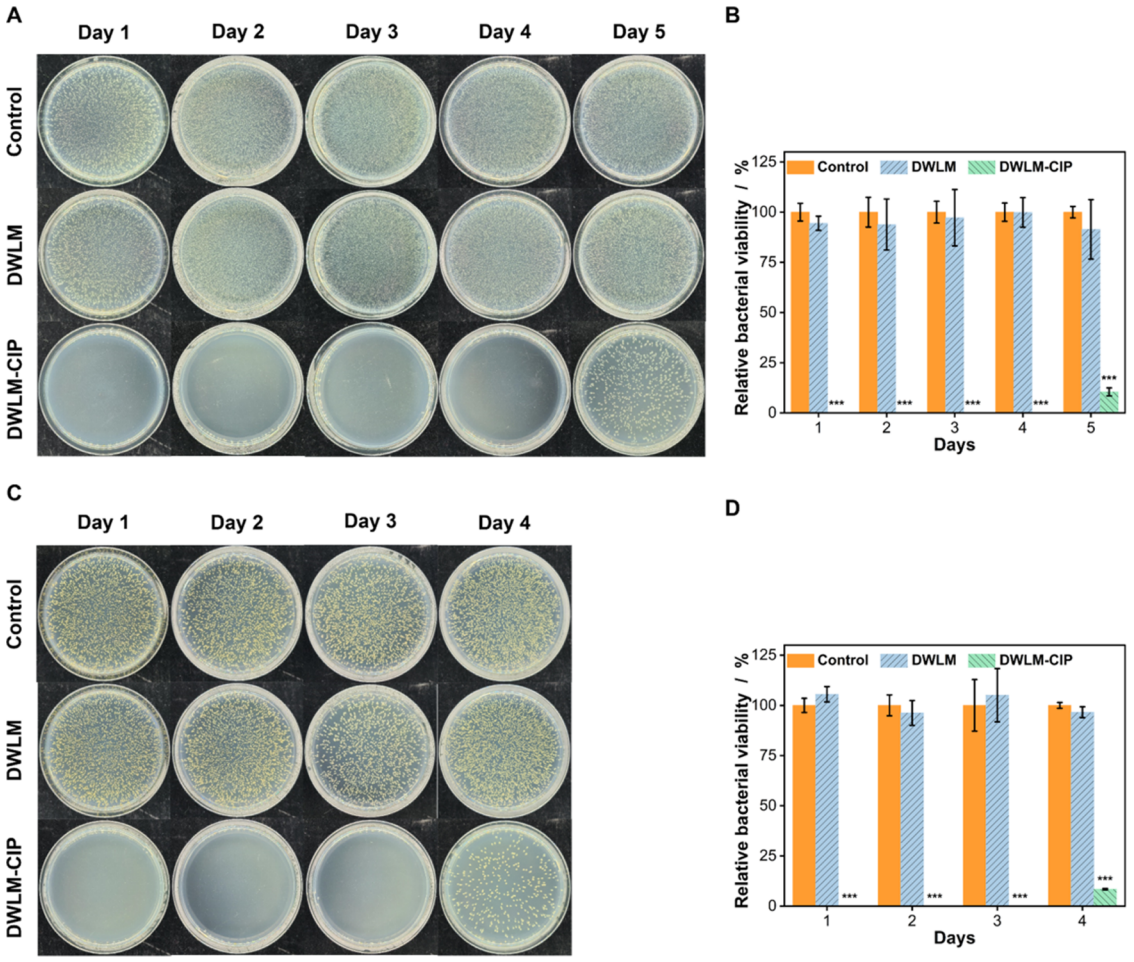

Figure 6. Long-lasting antibacterial activity of DWLM and DWLM-CIP. Photos of bacterial colonies and the corresponding bacterial viabilities formed by (A, B) *E. coli* and (C, D) *S. aureus* at different days. Values are expressed as the mean ± SD; $n = 3$.

The VPTT of the microgel was improved by the introduction of hydrophilic DWL, and pH-responsiveness was imparted to the microgel. Here, the pH-responsiveness of EM and DWLM was further evaluated by the DLS assay. Figure 1E illustrates the pH-dependent swelling of the microgels at 25 °C. The particle size ratios of EM at pH 3.1 to that at pH 10.0 and DWLM at pH 3.2 to that at pH 10.0 were defined as the swelling ratio, which were 1.22 (197.7 ± 3.7 nm/162.2 ± 5.5 nm) and 1.50 (579.7 ± 15.6 nm/386.6 ± 4.8 nm), respectively. As expected, pH-induced swelling of DWLM was significant. The size of the DWLM increases with increasing pH. The change in surface charge with the pH of DWLM was also investigated by ζ-potential measurement (Figure 1F). The ζ-potential values of DWLM were almost constant at pH values from 3.2 to 3.9 and at pH values from 8.1 to 10.0 with values of approximately −22.5 ± 0.8 and −40.3 ± 1.6 mV, respectively. As the pH of the medium increased, the carboxyl groups in the DWL became more ionized. The repulsion between the carboxylate anions causes swelling and increases the size of the microgel.[31] The above results demonstrate the pH-responsiveness of the DWLM.

3.2. CIP Loading of DWLM-CIP. In this experiment, ciprofloxacin hydrochloride (CIP) was chosen as the model drug for microgel encapsulation. Briefly, drug loading was achieved by combining CIP with the microgel dispersion and stirring for 24 h at 4 °C. The microgel obtained was named DWLM-CIP. When CIP is loaded into the microgel by physical adsorption, interactions between the microgel and CIP may occur. Specifically, hydrogen bonds may form between the $-COO^-$ and −OH groups of deacetylated WL within the microgel and the −COOH and -NH- groups of CIP. This interaction could enable the CIP to be more efficiently embedded in the 3D network of the microgel. Following a 24 h loading period, the UV−vis spectrometer was used to measure the encapsulated CIP in microgels, while the encapsulation efficiency (EE) and the drug loading capacity (DLC) were calculated using eqs 1 and 2. The EE and DLC of CIP in DWLM-CIP were measured to be approximately 33.09 ± 0.37 and 2.96 ± 0.03%, respectively. Figure 2A displays the UV−vis spectrum of DWLM-CIP, in comparison to the spectra of DWLM and CIP. CIP exhibited adsorption peaks at approximately 276 nm. In addition, the characteristic absorption peaks of CIP were evident in the UV−vis spectra of DWLM-CIP, demonstrating successful CIP loading.[32] The morphology of synthesized DWLM-CIP was further observed by TEM, and as shown in Figure 2B, DWLM-CIP still retained a spherical structure with good dispersion. The particle size of DWLM-CIP (104.6 ± 12.3 nm, Table S1) was larger than that of DWLM (66.8 ± 14.9 nm), which might be due to the loading of CIP in DWLM-CIP. DLS was used to examine the effect of CIP loading on the size of the microgel. In the DLS size distribution (Figure 2C), the size of DWLM-CIP (688.8 ± 2.2 nm, PDI = 0.478 ± 0.03) was larger than that of DWLM (557.3 ± 2.6 nm in Figure 1A), indicating that loading the CIP

https://doi.org/10.1021/acsomega.4c07589
ACS Omega 2024, 9, 46397−46407

drug successfully led to an increase in the size of the DWLM-CIP.[33] Moreover, the ζ-potential of the DWLM was around −36.0 ± 1.1 mV, which was less than that of the DWLM-CIP (ca. −32.3 ± 1.4 mV) (Figure S3). The increased ζ-potential was attributed to the neutralization of the negative charge by a positively charged molecule, such as CIP.[34] The aforementioned characterization findings collectively validate the effective loading of DWLM-CIP with CIP.

3.3. *In Vitro* Drug Release Testing and Kinetic Studies. It is known that the pH of the gastrointestinal environment varies among different segments.[3] pH is a critical factor in oral drug delivery as it determines the release profile of loaded drugs in different microenvironments. Therefore, pH values of 3.0 and 6.8 were chosen to simulate gastric fluid and intestinal fluid.[27] The cumulative release profiles of CIP from DWLM-CIP at various pH levels were investigated by dialyzing DWLM-CIP against the corresponding pH buffer solutions at 37 °C. As shown in Figure 3A, there was an abrupt release of CIP during the first 15 min at all pH values studied. The release of CIP was higher at pH 6.8 (42.8 ± 2.0%) than at pH 3.0 (34.0 ± 0.7%). This result is attributed to the weak binding of the drug to the surface of the microgel.[35] Thereafter, the drug release rate decreased. During the 8 h period, the cumulative release of CIP was 43.3 ± 0.2 and 49.5 ± 0.3% in buffer solutions with pH levels of 3.0 and 6.8, respectively. The pK_a values of CIP are pK_{a1} = 6.18 and pK_{a2} = 8.8.[36] Due to the high solubility of CIP in acidic media, the release of CIP from DWLM-CIP at pH 3.0 may be higher than at pH 6.8.[36] However, Figure 3A shows that the pH-responsive release of CIP was the most effective at pH 6.8. This can be attributed to the fact that DWL chains exist mainly as carboxyl anions at higher pH, leading to Coulombic repulsion that results in the swelling of microgels and easy release of CIP.[5,6] Moreover, as shown in Figure S5A, the release rate of CIP from DWLM-CIP was significantly reduced, resulting in 47.1 ± 0.9% cumulative release at pH 3.0 and 52.3 ± 0.6% cumulative release at pH 6.8 over 48 h. Notably, the cumulative release of CIP after 48 h was not as high as expected, which may be attributed to two reasons. First, intramolecular and intermolecular hydrogen bonding between CIP (−COOH and -NH- groups) and DWL (−OH and $-COO^-$ groups) of the microgel could have occurred, potentially impeding drug release.[37] Second, the release temperature of 37 °C exceeded the VPTT (30 °C) of the microgel, potentially causing some degree of particle size collapse and thus reducing drug release. The drug release data at 20 °C (less than the VPTT) verified the second reason. As shown in Figure 3B, at 20 °C and a release time of 8 h, the cumulative release of CIP was 55.9 ± 0.6 and 59.2 ± 1.1% at pH 3.0 and 6.8, respectively. These values were higher than the cumulative release of CIP observed at 37 °C for 8 h, which was 43.3 ± 0.2% at pH 3.0 and 49.5 ± 0.3% at pH 6.8. This phenomenon relates to the increased swelling of the microgel at 20 °C, thereby facilitating the release of CIP. These results confirm the temperature responsiveness of CIP release from DWLM-CIP. Furthermore, at 48 h, the cumulative release of CIP at pH 3.0 was 58.1 ± 0.5% at 20 °C (Figure S5B), which was 11% higher than the 47.1 ± 0.9% at 37 °C. Thus, the simulated body temperature of 37 °C effectively reduces the release of CIP into the simulated gastric fluid at pH 3.0, compared to 20 °C, helping to reduce unnecessary drug leakage during oral administration.

The *in vitro* release kinetics of CIP from DWLM-CIP were studied by fitting drug release data for 48 h to four models. As shown in Table 1, the R^2 values obtained from the Korsmeyer−Peppas release rate at different temperatures for both pH values were nearly 1, suggesting that the drug release of CIP from DWLM-CIP followed the Korsmeyer−Peppas kinetic model. All release index (n) values were less than 0.5, suggesting that the release of CIP adhered to Fickian diffusion.[38,39]

3.4. *In Vitro* Cytocompatibility Assessment. In general, the drug-carrying system should not exhibit cytotoxicity. HEK293T is often selected as a model cell for evaluating the cytocompatibility of oral drug delivery vehicles due to its easy accessibility and rapid growth.[40,41] The cytotoxicity of DWLM, DWLM-CIP, and CIP was assessed by MTT assay.[13] Figure 4 shows the viability of human embryonic kidney 293T cells (HEK293T) after 24 h contact culture with the samples. No cytotoxic effects were observed in microgels (DWLM) without the drug. Conversely, at a concentration of 4 mg/mL, DWLM-CIP showed a cell viability of 75.9 ± 1.7%, whereas the viability of free CIP was significantly lower at 54.9 ± 1.0%. Reduced cytotoxicity was observed after drug loading on DWLM. Any decrease in viability greater than 30% was classified as cytotoxic according to ISO 10993-5.[42] Therefore, the above results show that DWLM-CIP has good biocompatibility and is suitable for various biomedical applications, such as serving as an oral drug carrier.

3.5. *In Vitro* Antibacterial Performance. The antibacterial activity of the microgel was evaluated *in vitro* against Gram-negative *E. coli* and Gram-positive *S. aureus*.[43] And none of the microgel samples showed cytotoxic effects on HEK293T in the tested concentration range. The inhibitory zone test was carried out first. After the samples were co-cultured with bacteria for 24 h, the inhibition zones formed around the wells were measured and photographed. As shown in Figure 5A, the antibacterial zone diameters of DWLM, DWLM-CIP, and CIP against *E. coli* were 0, 3.1, and 3.5 cm, respectively. Meanwhile, the antibacterial zone diameters against *S. aureus* were 0, 3.0, and 3.3 cm, respectively (Figure 5B). These results indicated that DWLM had no antibacterial activity against any of the bacteria, whereas DWLM-CIP inhibited the bacterial growth. Thus, the antibacterial activity of DWLM-CIP is attributed to only the drug released from the microgel. Furthermore, the data showed that CIP was more effective in killing and inhibiting *E. coli* than *S. aureus*, resulting in a greater inhibition area for *E. coli*.[44] The antibacterial activity of DWLM-CIP was slightly lower than that of CIP, probably because of the limited drug release from the microgel.[38]

In a previous study, drug release from DWLM-CIP was found to plateau within 8 h. The efficacy of DWLM, DWLM-CIP, and CIP against *E. coli* and *S. aureus* were then evaluated to determine their antibacterial activity. Bacteria were treated with various concentrations of samples for 8 h, recultured on agar plates, and evaluated by bacterial enumeration to determine bacterial growth inhibition. The numbers of *E. coli* and *S. aureus* colonies treated with DWLM-CIP and CIP decreased significantly with increasing concentrations. As shown in Figure 5C,D, at a concentration of 7.50 μg/mL, DWLM-CIP exhibited an over 99% inactivation of *E. coli*, a result comparable to that obtained with an equivalent concentration of CIP. Furthermore, at 15.00 μg/mL, DWLM-CIP also achieved over 99% inactivation of *S. aureus*, with results comparable to those obtained with an equivalent concentration of CIP (Figure 5E,F). Similarly, antimicrobial activity against *E. coli* and *S. aureus* was not demonstrated by

https://doi.org/10.1021/acsomega.4c07589
ACS Omega 2024, 9, 46397−46407

DWLM. The above results confirm the expected good antimicrobial activity of the designed DWLM-CIP.

In addition, DWLM and DWLM-CIP were cultured daily with the newly prepared bacterial suspensions to investigate their long-term antimicrobial activity (Figure 6). It was observed that DWLM-CIP at 1 mg/mL significantly inhibited *E. coli* growth for up to 4 days; while, at 4 mg/mL, it effectively suppressed *S. aureus* growth for up to 3 days. The sustained release of the drug may be responsible for the long-term antimicrobial properties of the microgel. The antimicrobial results presented above show that DWLM-CIP has excellent antibacterial activity.

4. CONCLUSIONS

In summary, our work is dedicated to the development and characterization of DWLM as an oral drug carrier. Using physical adsorption, we successfully incorporated the model drug CIP into the DWLM to prepare DWLM-CIP. DLS results showed that DWLM exhibited dual responsiveness to temperature and pH. The release profiles of CIP under simulated gastrointestinal conditions (pH 3.0 and 6.8) at 37 and 20 °C confirmed the pH and temperature responsiveness of drug release from DWLM-CIP, consistent with the Korsmeyer–Peppas kinetic model. The cumulative release of CIP was 6.2% higher at pH 6.8 (49.5 ± 0.3%) than at pH 3.0 (43.3 ± 0.2%) after 8 h of release at 37 °C. MTT assay results indicated that HEK293T viability was 75.9 ± 1.7% at a DWLM-CIP concentration of 4 mg/mL. The HEK293T viability of CIP at the same concentration was only 54.9 ± 1.0%, indicating that DWLM-CIP has good biocompatibility. Antimicrobial testing showed that DWLM-CIP retained effective long-term antimicrobial activity against both *E. coli* and *S. aureus* for 4 and 3 days, respectively. These collective results indicate that the fabricated DWL-based microgel drug delivery system serves as an improved model for the oral delivery of CIP. Furthermore, this work establishes a strong basis for the fabrication and application of DWL in the field of micro/nanomaterials.

■ ASSOCIATED CONTENT

Supporting Information

The Supporting Information is available free of charge at https://pubs.acs.org/doi/10.1021/acsomega.4c07589.

UV–vis standard curves of CIP in different solutions; photos of EM dilute dispersions at 17 and 27 °C; photos of DWLM dilute dispersions at 22 and 37 °C; ζ-potentials of DWLM and DWLM-CIP at 25 °C; the cumulative release of CIP from DWLM-CIP at different pH values at 37 and 20 °C over 48 h; size of DWLM and DWLM-CIP under TEM. (PDF)

■ AUTHOR INFORMATION

Corresponding Authors

Aiping Chang − *Fujian-Taiwan Science and Technology Cooperation Base of Biomedical Materials and Tissue Engineering, Engineering Research Center of Industrial Biocatalysis, Fujian Provincial Key Laboratory of Advanced Materials Oriented Chemical Engineering, Fujian Provincial Key Laboratory of Polymer Materials, College of Chemistry and Materials Science, Fujian Normal University, Fuzhou 350117, People's Republic of China*; Phone: +86-591-22860021; Email: aipingchang@fjnu.edu.cn

Hu Zhu − *Fujian-Taiwan Science and Technology Cooperation Base of Biomedical Materials and Tissue Engineering, Engineering Research Center of Industrial Biocatalysis, Fujian Provincial Key Laboratory of Advanced Materials Oriented Chemical Engineering, Fujian Provincial Key Laboratory of Polymer Materials, College of Chemistry and Materials Science, Fujian Normal University, Fuzhou 350117, People's Republic of China*; orcid.org/0000-0002-8359-3758; Phone: +86-591-22860021; Email: zhuhu@fjnu.edu.cn

Authors

Zhenyin Huang − *Fujian-Taiwan Science and Technology Cooperation Base of Biomedical Materials and Tissue Engineering, Engineering Research Center of Industrial Biocatalysis, Fujian Provincial Key Laboratory of Advanced Materials Oriented Chemical Engineering, Fujian Provincial Key Laboratory of Polymer Materials, College of Chemistry and Materials Science, Fujian Normal University, Fuzhou 350117, People's Republic of China*

Hanyu Dong − *Fujian-Taiwan Science and Technology Cooperation Base of Biomedical Materials and Tissue Engineering, Engineering Research Center of Industrial Biocatalysis, Fujian Provincial Key Laboratory of Advanced Materials Oriented Chemical Engineering, Fujian Provincial Key Laboratory of Polymer Materials, College of Chemistry and Materials Science, Fujian Normal University, Fuzhou 350117, People's Republic of China*

Yingjie Qiu − *Fujian-Taiwan Science and Technology Cooperation Base of Biomedical Materials and Tissue Engineering, Engineering Research Center of Industrial Biocatalysis, Fujian Provincial Key Laboratory of Advanced Materials Oriented Chemical Engineering, Fujian Provincial Key Laboratory of Polymer Materials, College of Chemistry and Materials Science, Fujian Normal University, Fuzhou 350117, People's Republic of China*

Complete contact information is available at: https://pubs.acs.org/10.1021/acsomega.4c07589

Author Contributions

H.Z. and A.C.: Conceptualization. Z.H. and A.C.: Investigation and writing—original draft. H.D. and Y.Q.: Data curation. H.Z. and A.C.: Writing—review and editing. All authors have read and agreed to the published version of the manuscript.

Notes

The authors declare no competing financial interest.

■ ACKNOWLEDGMENTS

This work was financially supported by the Natural Science Foundation of China (grant no. U1805234), Natural Science Foundation of Fujian Province of China (grant no. 2023H6011), Program for Innovative Research Team in Science and Technology in Fujian Province University, 100 Talents Program of Fujian Province, Fujian-Taiwan Science and Technology Cooperation Base of Biomedical Materials and Tissue Engineering (grant no. 2021D039), Fu-Xia-Quan National Independent Innovation Demonstration Zone Collaborative Innovation Platform Project (2022FX3), and Fujian Provincial Major Project for Young and Middle-aged Scientific Research in Health and Wellness (2023ZQNZD020).

https://doi.org/10.1021/acsomega.4c07589
ACS Omega 2024, 9, 46397−46407

■ ABBREVIATIONS

WL:sphingan WL gum; DWL:deacetylated sphingan WL gum; PEGMA:poly[oligo(ethylene glycol)methacrylate]; SDS:sodium dodecyl sulfate; APS:ammonium persulfate; CIP:ciprofloxacin hydrochloride; DWLM:DWL-based microgels; DWLM-CIP:DWLM with the loaded CIP; MTT:methyl thiazolyl tetrazolium; HEK293T:human embryonic kidney cells 293T; PDI:polydispersity index; DLS:dynamic light scattering; FTIR:Fourier transform infrared spectroscopy; UV−vis:ultraviolet−visible absorption spectroscopy; TEM:-transmission electron microscopy

■ REFERENCES

(1) Wang, Y.; Guo, L.; Dong, S.; Cui, J.; Hao, J. Microgels in biomaterials and nanomedicines. *Adv. Colloid Interface Sci.* **2019**, *266*, 1−20.

(2) Plamper, F. A.; Richtering, W. Functional Microgels and Microgel Systems. *Acc. Chem. Res.* **2017**, *50* (2), 131−140.

(3) Yang, Z.; McClements, D. J.; Li, C.; Sang, S.; Chen, L.; Long, J.; Qiu, C.; Jin, Z. Targeted delivery of hydrogels in human gastrointestinal tract: A review. *Food Hydrocolloids* **2023**, *134*, 108013.

(4) Hajebi, S.; Rabiee, N.; Bagherzadeh, M.; Ahmadi, S.; Rabiee, M.; Roghani-Mamaqani, H.; Tahriri, M.; Tayebi, L.; Hamblin, M. R. Stimulus-responsive polymeric nanogels as smart drug delivery systems. *Acta Biomater.* **2019**, *92*, 1−18.

(5) Bai, Y.; Zhang, Z.; Deng, M.; Chen, L.; He, C.; Zhuang, X.; Chen, X. Thermo- and pH-responsive microgels for controlled release of insulin. *Polym. Int.* **2012**, *61* (7), 1151−1157.

(6) Rashid, Z.; Ranjha, N. M.; Rashid, F.; Raza, H. Pharmacokinetic evaluation of microgels for targeted and sustained delivery of acid labile active pharmaceutical agent in animal model. *J. Drug Delivery Sci. Technol.* **2020**, *57*, 101770.

(7) Li, H.; Jiao, X.; Sun, Y.; Sun, S.; Feng, Z.; Zhou, W.; Zhu, H. The preparation and characterization of a novel sphingan WL from marine Sphingomonas sp. WG. *Sci. Rep.* **2016**, *6* (1), No. 37899, DOI: 10.1038/srep37899.

(8) Li, H.; Feng, Z.-m.; Sun, Y.-j.; Zhou, W.-l.; Jiao, X.; Zhu, H. Draft Genome Sequence of *Sphingomonas sp. WG*, a Welan Gum-Producing Strain. *Genome Announcements* **2016**, *4* (1), No. e01709-15, DOI: 10.1128/genomeA.01709-15.

(9) Kaur, V.; Bera, M. B.; Panesar, P. S.; Kumar, H.; Kennedy, J. F. Welan gum: Microbial production, characterization, and applications. *Int. J. Biol. Macromol.* **2014**, *65*, 454−461.

(10) Chang, A.; Ye, Z.; Ye, Z.; Deng, J.; Lin, J.; Wu, C.; Zhu, H. Citric acid crosslinked sphingan WL gum hydrogel films supported ciprofloxacin for potential wound dressing application. *Carbohydr. Polym.* **2022**, *291*, 119520.

(11) Lin, J.; Deng, J.; Huang, Z.; Dong, H.; Chang, A.; Zhu, H. Physicochemical and Structural Characterization of Alkali-Treated Biopolymer Sphingan WL Gum from Marine *Sphingomonas sp. WG*. *ACS Omega* **2023**, *8* (7), 7163−7171.

(12) Li, H.; Li, J.; Jiao, X.; Li, K.; Sun, Y.; Zhou, W.; Shen, Y.; Qian, J.; Chang, A.; Wang, J.; Zhu, H. Characterization of the biosynthetic pathway of nucleotide sugar precursor UDP-glucose during sphingan WL gum production in Sphingomonas sp. WG. *J. Biotechnol.* **2019**, *302*, 1−9.

(13) Ji, S.; Li, H.; Wang, G.; Lu, T.; Ma, W.; Wang, J.; Zhu, H.; Xu, H. Rheological behaviors of a novel exopolysaccharide produced by Sphingomonas WG and the potential application in enhanced oil recovery. *Int. J. Biol. Macromol.* **2020**, *162*, 1816−1824.

(14) Ji, S.; Li, H.; Xue, H.; Guo, Z.; Liu, J.; Chen, M.; Wang, J.; Zhu, H.; Xu, H. Effects of monosaccharide composition and acetyl content on the rheological properties of sphingan WL. *Colloids Surf., A* **2022**, *650*, 129609.

(15) Deng, J.; Lin, J.; Huang, Z.; Xu, X.; Chang, A.; Zhu, H. Preparation and properties of marine-derived sphingan WL gum-metal ion composite hydrogels. *Colloid Polym. Sci.* **2023**, *301* (9), 1115−1124.

(16) Li, H.; Li, K.; Guo, Z.; Xue, H.; Li, J.; Ji, S.; Wang, J.; Zhu, H. The Function of β-1,4-Glucuronosyltransferase WelK in the Sphingan WL Gum Biosynthesis Process in Marine Sphingomonas sp. WG. *Mar. Biotechnol.* **2021**, *23* (1), 39−50.

(17) Mauri, E.; Giannitelli, S. M.; Trombetta, M.; Rainer, A. Synthesis of Nanogels: Current Trends and Future Outlook. *Gels* **2021**, *7* (2), No. 36.

(18) Chiriac, A. P.; Ghilan, A.; Neamtu, I.; Nita, L. E.; Rusu, A. G.; Chiriac, V. M. Advancement in the Biomedical Applications of the (Nano)gel Structures Based on Particular Polysaccharides. *Macromol. Biosci.* **2019**, *19* (9), No. 1900187, DOI: 10.1002/mabi.201900187.

(19) Debele, T. A.; Mekuria, S. L.; Tsai, H.-C. Polysaccharide based nanogels in the drug delivery system: Application as the carrier of pharmaceutical agents. *Mater. Sci. Eng. C* **2016**, *68*, 964−981.

(20) Li, C.; Obireddy, S. R.; Lai, W.-F. Preparation and use of nanogels as carriers of drugs. *Drug Delivery* **2021**, *28* (1), 1594−1602.

(21) Tehrani, S. M.; Lu, Y.; Winnik, M. A. PEGMA-Based Microgels: A Thermoresponsive Support for Enzyme Reactions. *Macromolecules* **2016**, *49* (22), 8711−8721.

(22) Uhljar, L. É.; Kan, S. Y.; Radacsi, N.; Koutsos, V.; Szabó-Révész, P.; Ambrus, R. In Vitro Drug Release, Permeability, and Structural Test of Ciprofloxacin-Loaded Nanofibers. *Pharmaceutics* **2021**, *13* (4), No. 556.

(23) Hosseini-Ashtiani, N.; Tadjarodi, A.; Zare-Dorabei, R. Low molecular weight chitosan-cyanocobalamin nanoparticles for controlled delivery of ciprofloxacin: Preparation and evaluation. *Int. J. Biol. Macromol.* **2021**, *176*, 459−467.

(24) Prusty, K.; Biswal, A.; Biswal, S. B.; Swain, S. K. Synthesis of soy protein/polyacrylamide nanocomposite hydrogels for delivery of ciprofloxacin drug. *Mater. Chem. Phys.* **2019**, *234*, 378−389.

(25) Li, H.; Mergel, O.; Jain, P.; Li, X.; Peng, H.; Rahimi, K.; Singh, S.; Plamper, F. A.; Pich, A. Electroactive and degradable supramolecular microgels. *Soft Matter* **2019**, *15* (42), 8589−8602.

(26) Cai, S.; Li, X.; Pu, S.; Ma, X.; He, X. Preparation of poly(acrylamide-co-Acrylonitrile) thermosensitivity microgel and control release of aspirin. *Int. J. Polym. Mater. Polym. Biomater.* **2023**, *72* (14), 1142−1150.

(27) Li, X.; Hetjens, L.; Wolter, N.; Li, H.; Shi, X.; Pich, A. Charge-reversible and biodegradable chitosan-based microgels for lysozyme-triggered release of vancomycin. *J. Adv. Res.* **2023**, *43*, 87−96.

(28) Wu, S.; Gong, Y.; Liu, S.; Pei, Y.; Luo, X. Functionalized phosphorylated cellulose microspheres: Design, characterization and ciprofloxacin loading and releasing properties. *Carbohydr. Polym.* **2021**, *254*, 117421.

(29) Che, Y.; Li, D.; Liu, Y.; Yue, Z.; Zhao, J.; Ma, Q.; Zhang, Q.; Tan, Y.; Yue, Q.; Meng, F. Design and fabrication of a triple-responsive chitosan-based hydrogel with excellent mechanical properties for controlled drug delivery. *J. Polym. Res.* **2018**, *25* (8), No. 169, DOI: 10.1007/s10965-018-1568-5.

(30) Zhang, J. T.; Pan, C. J.; Keller, T.; Bhat, R.; Gottschaldt, M.; Schubert, U. S.; Jandt, K. D. Monodisperse, Temperature-Sensitive Microgels Crosslinked by Si-O-Si Bonds. *Macromol. Mater. Eng.* **2009**, *294* (6−7), 396−404.

(31) Li, J.; Lu, Z.; Chen, Z.; Li, C.; Du, Y.; Chen, C.; Wang, L.; Yu, P. Preparation and characterization of pH-responsive microgel using arabinoxylan from wheat bran for BSA delivery. *Food Chem.* **2021**, *342*, 128220.

(32) Zhang, H.; Pei, M.; Liu, P. pH-Activated surface charge-reversal double-crosslinked hyaluronic acid nanogels with feather keratin as multifunctional crosslinker for tumor-targeting DOX delivery. *Int. J. Biol. Macromol.* **2020**, *150*, 1104−1112.

(33) Gao, D.; Duan, L.; Wu, M.; Wang, X.; Sun, Z.; Zhang, Y.; Li, Y.; He, P. Preparation of thermo/redox/pH-stimulative poly(N-isopropylacrylamide-co-N,N′-dimethylaminoethyl methacrylate) nanogels and their DOX release behaviors. *J. Biomed. Mater. Res., Part A* **2019**, *107* (6), 1195−1203.

https://doi.org/10.1021/acsomega.4c07589
ACS Omega 2024, 9, 46397−46407

(34) Watcharadulyarat, N.; Rattanatayarom, M.; Ruangsawasdi, N.; Patikarnmonthon, N. PEG−PLGA nanoparticles for encapsulating ciprofloxacin. *Sci. Rep.* **2023**, *13* (1), No. 266, DOI: 10.1038/s41598-023-27500-y.
(35) Naranjo, A. G.; Cobas, H. V.; Gupta, N. K.; Rodríguez López, K.; Peña, A. A.; Sacasas, D.; Brito, R. A. 5-Fluorouracil uptake and release from pH-responsive nanogels: An experimental and computational study. *J. Mol. Liq.* **2022**, *362*, 119716.
(36) Sayyar, Z.; Mahdavinia, G. R.; Khataee, A. Dual-drug (Curcumin/Ciprofloxacin) loading and release from chitosan-based hydrogels embedded with magnetic Montmorillonite/Hyaluronic acid for enhancing wound healing. *J. Biol. Eng.* **2023**, *17* (1), No. 66, DOI: 10.1186/s13036-023-00385-1.
(37) Mahmud, M.; Salem, K. S.; Bari, M. L.; Qiu, H. Architecting Ultrathin Graphitic C3N4 Nanosheets Incorporated PVA/Gelatin Bionanocomposite for Potential Biomedical Application: Effect on Drug Delivery, Release Kinetics, and Antibacterial Activity. *ACS Appl. Bio Mater.* **2022**, *5*, 5126−5139.
(38) Esim, O.; Kiymaci, M. E.; Hascicek, C. Ciprofloxacin HCl-loaded Albumin Nanoparticles for the Treatment of Recurrent Urinary Tract Infections: Preparation, Optimization, and Evaluation of Antibacterial Activity. *J. Pharm. Innovation* **2023**, *18* (3), 1100−1110.
(39) Hajebi, S.; Abdollahi, A.; Roghani-Mamaqani, H.; Salami-Kalajahi, M. Hybrid and hollow Poly(N,N-dimethylaminoethyl methacrylate) nanogels as stimuli-responsive carriers for controlled release of doxorubicin. *Polymer* **2019**, *180*, 121716.
(40) Shi, Y.; Xue, J.; Xu, S.; You, Y.; Yan, X. Q.; Zhao, X.; Cao, J. Polyelectrolyte complex nanoparticles based on chitosan and methoxy poly(ethylene glycol) methacrylate-co-poly(methylacrylic acid) for oral delivery of ibuprofen. *Colloids Surf., B* **2018**, *165*, 235−242.
(41) Durán-Lobato, M.; Martín-Banderas, L.; Lopes, R.; Gonçalves, L. M. D.; Fernández-Arévalo, M.; Almeida, A. J. Lipid nanoparticles as an emerging platform for cannabinoid delivery: physicochemical optimization and biocompatibility. *Drug Dev. Ind. Pharm.* **2016**, *42* (2), 190−198.
(42) Wu, D.-Q.; Cui, H.-C.; Zhu, J.; Qin, X.-H.; Xie, T. Novel amino acid based nanogel conjugated suture for antibacterial application. *J. Mater. Chem. B* **2016**, *4* (15), 2606−2613.
(43) Jabbari, P.; Mahdavinia, G. R.; Rezaei, P. F.; Heragh, B. K.; Labib, P.; Jafari, H.; Javanshir, S. pH-responsive magnetic biocompatible chitosan-based nanocomposite carrier for ciprofloxacin release. *Int. J. Biol. Macromol.* **2023**, *250*, 126228.
(44) Aden, S. F.; Mahmoud, L. A. M.; Ivanovska, E. H.; Terry, L. R.; Ting, V. P.; Katsikogianni, M. G.; Nayak, S. Controlled delivery of ciprofloxacin using zirconium-based MOFs and poly-caprolactone composites. *J. Drug Delivery Sci. Technol.* **2023**, *88*, 104894.

https://doi.org/10.1021/acsomega.4c07589
ACS Omega 2024, 9, 46397−46407